

# Disorder effects in a model of competing superconducting and charge-density wave orders in $\text{YBa}_2\text{Cu}_3\text{O}_{6+x}$

Dror Orgad

*Racah Institute of Physics, The Hebrew University, Jerusalem 91904, Israel*

(Dated: January 14, 2025)

There is evidence for competition between superconductivity and short-range charge-density wave order in a number of cuprate compounds and especially in  $\text{YBa}_2\text{Cu}_3\text{O}_{6+x}$ . Here, we use a non-linear sigma model of such competition to study the effects of spatially correlated disorder in the chain layers and delta-correlated disorder in the  $\text{CuO}_2$  layers. The first is relevant to the oxygen ortho structure and the latter may be induced by electron irradiation. We find that reducing the correlation length of the potential on the chain layers decreases the size of the charge-density wave structure factor but has little effect on its temperature dependence, as observed experimentally. At the same time, the charge-density-wave correlation length decreases more than is seen in the experiment. The temperature at which the structure factor peaks coincides with  $T_c$  and both decrease when disorder is introduced into the  $\text{CuO}_2$  planes. Strengthening this disorder reduces the magnitude of the structure factor and eventually turns it into a monotonic function of the temperature. This occurs despite an increase in the local magnitude of the charge-density wave order.

## I. INTRODUCTION

Signatures of short-range charge-density wave (CDW) order have been detected in a wide range of cuprate superconductors [1–22]. The short-range CDW appears to compete with superconductivity and in  $\text{YBa}_2\text{Cu}_3\text{O}_{6+x}$  (YBCO) it is possible to stabilize a much longer-ranged order with the same incommensurate wavelength by suppressing superconductivity using either strong magnetic fields, [23–29] or strain [30–32]. Another agent that is capable of tipping the balance between the two ordering tendencies is the disorder present in any physical sample.

Previous works have introduced Ginzburg-Landau and nonlinear sigma models (NLSM) to study the competition between superconducting and CDW orders in the absence [33–36] and presence of disorder [32, 37–39]. In particular, we have shown that increasing the strength of a delta-correlated Gaussian disorder leads to larger short-range CDW correlations at low temperatures [38]. If interpreted as a universal relation between disorder strength and CDW correlations this appears to conflict with an experiment by Achkar *et al.* [40], who used quench cooling to destroy the ortho structure of the doped oxygens in the YBCO chain layers [41] and resonant x-ray scattering to reveal that such disordering of the dopant atoms leads to uniform *reduction* of the CDW structure factor across all temperatures.

Our studies of an NLSM adopted to reflect the structure of YBCO have demonstrated its ability to reproduce many of the salient features of the observed CDW signatures in this compound under the influence of magnetic fields [39] and strain [32]. However, while these works included a random potential on the chain layers, we have not yet investigated the effects of varying the correlation length of the potential. Hence, it remains uncertain whether the same NLSM can also capture the observed reduction in the CDW correlations due to oxygen disordering. In the following we answer this question in the affirmative using numerical Monte Carlo simulations.

Specifically, we show that increasing the correlation length of the potential in the chain layers induces an increase in the CDW structure factor, even when the variance of the random potential is simultaneously reduced. This indicates that a correlated chain potential is more effective in nucleating CDW order than a local Gaussian disorder. Furthermore, the relative increase in the CDW structure factor is largely independent of the temperature, as was observed experimentally [40]. Similar statements hold for the magnitude and temperature dependence of the calculated CDW correlation length. Here, however, we find a discrepancy with the experimental results [40] that exhibit considerably smaller changes in the magnitude of the CDW correlation length following the disordering of the ortho structure. Given the overall success of the model in reproducing the observed phenomenology, I take this discrepancy as a guidance for further theoretical refinements.

In YBCO, disorder naturally arises from oxygen doping and is mostly confined to the chain layers. However, it is possible to introduce point defects directly into the  $\text{CuO}_2$  planes by electron irradiation [42]. This raises the intriguing question of how such disorder influences the interplay between the CDW correlations and superconductivity. We have not addressed this issue before within our model, nor are we familiar with relevant experiments on YBCO. To fill the gap and provide a theoretical reference point for future experiments we describe below our findings regarding the behavior of the NLSM with additional Gaussian disorder on the  $\text{CuO}_2$  planes. We show that although the additional disorder *enhances* the amplitude of the local CDW order it causes a *reduction* in the size of the CDW structure factor owing to a decrease in the CDW correlation length. It also affects the temperature dependence of the structure factor, which for not too strong disorder exhibits a peak at the superconducting  $T_c$ . Increasing the disorder reduces  $T_c$  and eventually turns the structure factor into a monotonically decreasing function of the temperature.

Finally, and from a more analytical perspective, we aim to explore the extent to which the properties of the disordered NLSM can be accurately captured by the large- $N$  approximation ( $N$  being the number of components of the vector of order parameters). We show that while the saddle-point equations (infinite- $N$  limit) reproduce the broad qualitative features of the physical model, they miss some of the quantitative aspects. Including  $1/N$  corrections into the analysis improves the quantitative agreement at high temperature but introduces increased deviations in the vicinity of  $T_c$ .

## II. THE MODEL

We consider a model consisting of  $L_z/2$  bilayers representing the  $\text{CuO}_2$  bilayers of YBCO. Each layer hosts a three-dimensional complex order parameter whose components correspond to a superconducting order parameter  $\psi_{j\mu}(\mathbf{r})$ , and two complex CDW order parameters  $\Phi_{j\mu}^{a,b}(\mathbf{r})$ . The latter describe density variations  $\delta\rho_{j\mu}(\mathbf{r}) = e^{i\mathbf{Q}_a \cdot \mathbf{r}} \Phi_{j\mu}^a(\mathbf{r}) + e^{i\mathbf{Q}_b \cdot \mathbf{r}} \Phi_{j\mu}^b(\mathbf{r}) + \text{c.c.}$  along the crystallographic  $a$  and  $b$  directions with incommensurate wave-vectors  $\mathbf{Q}_{a,b}$ . Here,  $\mu = 0, 1$  denotes the bottom (top) layer within a bilayer, which by itself is indexed by  $j$ . In the following we coarse grain the planes, such that the in-plane position vector  $\mathbf{r}$  corresponds to sites on a square lattice whose lattice constant  $a$  is the observed CDW period, i.e., about three Cu-Cu spacings.

We focus on temperatures below the onset temperature of short-range CDW correlations (135-155K in YBCO) and assume the existence of some type of local order at every lattice point. The competition between the different components is encapsulated by the constraints

$$|\psi_{j\mu}(\mathbf{r})|^2 + |\Phi_{j\mu}(\mathbf{r})|^2 = 1, \quad (1)$$

where  $\Phi_{j\mu} = (\Phi_{j\mu}^a, \Phi_{j\mu}^b)^T$ . The Hamiltonian is

$$\begin{aligned} H = & \sum_j \sum_{\mu=0,1} H_{j\mu} + \frac{\rho_s}{2} \sum_j \sum_{\mathbf{r}} \left[ \tilde{U} \Phi_{j,0}^\dagger \Phi_{j,1} \right. \\ & + U \Phi_{j,1}^\dagger \Phi_{j+1,0} - \tilde{J} \psi_{j,0}^* \psi_{j,1} - J \psi_{j,1}^* \psi_{j+1,0} \\ & \left. + \mathbf{V}_j^\dagger (\Phi_{j,1} + \Phi_{j+1,0}) + \text{c.c.} \right]. \quad (2) \end{aligned}$$

Henceforth, the bare superconducting stiffness,  $\rho_s$ , and the lattice constant  $a$  are set to 1 and serve as the basic energy and length scales. We model the Coulomb interaction between CDW fields within a bilayer by a local coupling  $\tilde{U}$ , and denote the intra-bilayer Josephson tunneling amplitude by  $\tilde{J}$ . The (weaker) Coulomb interaction and Josephson coupling between nearest-neighbor planes belonging to consecutive bilayers are denoted by  $U$  and  $J$ , respectively.

The last term in Eq. (2) describes the coupling between the disordered doped oxygens on the chain layers and the CDW fields on the adjacent bilayers. This

coupling may originate from local changes in the concentration of doped holes and from the Coulomb interaction between the oxygens and the CDW [22]. We model the chain potential via correlated random fields  $\mathbf{V}_j = (V_j^1 + iV_j^2, V_j^3 + iV_j^4)^T$  satisfying  $\overline{\mathbf{V}_j^\alpha(\mathbf{r})} = 0$  and

$$\overline{V_j^\alpha(\mathbf{r}) V_{j'}^\beta(\mathbf{r}')} = V^2 \delta_{\alpha\beta} \delta_{jj'} e^{-(|x-x'|+|y-y'|)/\xi_{\text{dis}}}, \quad (3)$$

with the overline signifying disorder averaging. Note that a similar linear coupling between the superconducting order  $\psi$  and the random fields is forbidden by gauge invariance. Therefore,  $\psi$  couples to the potentials only indirectly through the constraints, Eq. (1).

Within a layer the Hamiltonian reads

$$\begin{aligned} H_{j\mu} = & \frac{\rho_s}{2} \sum_{\mathbf{r}} \left[ |\nabla \psi_{j\mu}|^2 + \lambda |\nabla \Phi_{j\mu}|^2 + g |\tilde{\Phi}_{j\mu}|^2 \right. \\ & \left. + (\tilde{V}_{j\mu}^\dagger \Phi_{j\mu} + \text{c.c.}) \right], \quad (4) \end{aligned}$$

where  $\nabla$  is the discrete gradient,  $\lambda\rho_s$  is the CDW stiffness and  $g\rho_s$  is the effective CDW mass reflecting the energetic penalty for CDW ordering. The presence of such a penalty ensures that superconductivity prevails over the CDW order at  $T = 0$ , at least in the disorder-free regions. Finally,  $\tilde{\mathbf{V}}_{j\mu} = (\tilde{V}_j^1 + i\tilde{V}_j^2, \tilde{V}_j^3 + i\tilde{V}_j^4)^T$  is the disorder potential on the  $\text{CuO}_2$  layers, which we model by Gaussian random fields with zero mean and

$$\overline{\tilde{V}_{j\mu}^\alpha(\mathbf{r}) \tilde{V}_{j'\mu'}^\beta(\mathbf{r}')} = \tilde{V}^2 \delta_{\alpha\beta} \delta_{jj'} \delta_{\mu\mu'} \delta_{\mathbf{r}\mathbf{r}'}. \quad (5)$$

## III. MONTE CARLO RESULTS

We have used Monte Carlo simulations to study the model on an  $L \times L \times L_z$  lattice, and in particular to calculate the CDW structure factor

$$\begin{aligned} S_\alpha(\mathbf{q}, l) = & \frac{2}{L^2 L_z} \sum_{\mathbf{r}\mathbf{r}'} \sum_{jj'} \sum_{\mu\mu'} e^{-i[\mathbf{q} \cdot (\mathbf{r}-\mathbf{r}') + 2\pi(j-j' + \frac{\mu-\mu'}{3})l]} \\ & \times \langle \Phi_{j\mu}^\alpha(\mathbf{r}) \Phi_{j'\mu'}^{\alpha*}(\mathbf{r}') \rangle, \quad (6) \end{aligned}$$

where the averaging is over both thermal fluctuations and disorder realizations. The in-plane wave-vector  $\mathbf{q}$  in Eq. (6) is measured relative to  $\mathbf{Q}_{a,b}$ , and the expression for  $S_\alpha$  reflects the fact that in YBCO the  $\text{CuO}_2$  planes within a bilayer are separated by approximately  $1/3$  of the  $c$  axis lattice constant.

### A. Correlated chain layer potential

We begin by examining the consequences of varying the correlation length of the chain layer potential. Specifically, we compare the case with  $\xi_{\text{dis}} = 2$ , which corresponds to the reported correlation length in the ordered ortho samples of Ref. [40], and a system with  $\xi_{\text{dis}} = 0.2$ , which essentially lacks any spatial disorder correlations.

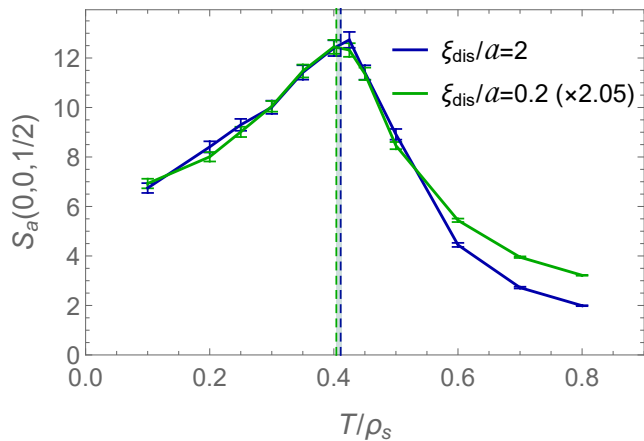


FIG. 1. The temperature dependence of the peak amplitude  $S_a(0,0,1/2)$  for a  $32^3$  system with  $V^2 = 0.035$ ,  $\xi_{\text{dis}} = 2$  (blue) and  $V^2 = 0.35$ ,  $\xi_{\text{dis}} = 0.2$  (green). In both cases  $\tilde{V}^2 = 0$ . The data for the system with  $\xi_{\text{dis}} = 0.2$  is scaled by a factor 2.05. The dashed vertical lines denote  $T_c$  for the two cases.

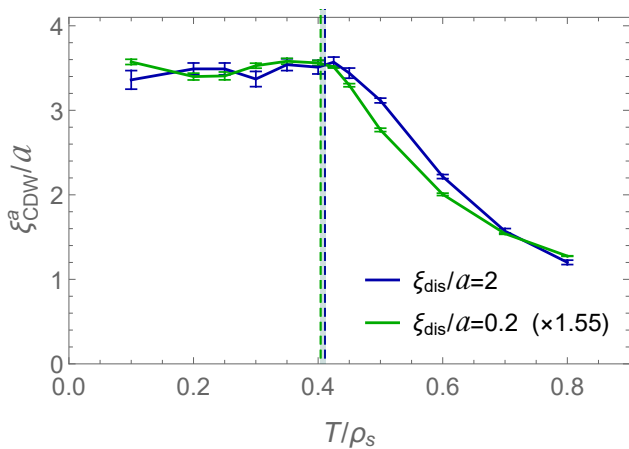


FIG. 2. The temperature dependence of the CDW correlation length for the same systems as in Fig. 1. The data for the system with  $\xi_{\text{dis}} = 0.2$  is scaled by a factor 1.55.

The correlated potential is generated from a Gaussian random field  $v$  via  $\mathcal{F}^{-1}[\mathcal{F}(v)\sqrt{\mathcal{F}(e^{-(|x|+|y|)/\xi_{\text{dis}}})}]$ , where  $\mathcal{F}$  denotes the Fourier transform. Each data point was typically averaged over 540 disorder realizations and throughout the simulations we have set  $\lambda = 1$ ,  $g = 1$ ,  $\tilde{U} = 0.85$ ,  $U = 0.12$ ,  $\tilde{J} = 0.15$ , and  $J = 0.015$ .

Figure 1 depicts the temperature dependence of the structure factor peak at  $\mathbf{Q}_a$  and  $l = 1/2$ . The peak amplitude increases as the temperature is lowered, attains a maximum at  $T_c$  (which we identify from the onset of superconducting order, see Fig. 3a) and then decreases below  $T_c$ . It remains finite down to zero temperature due to nucleation of CDW in domains that are dominated by the coupling to the chains potential, while superconductivity sets in within the intervening regions.

We find that a correlated chain potential is more effective in establishing coherent CDW order. For exam-

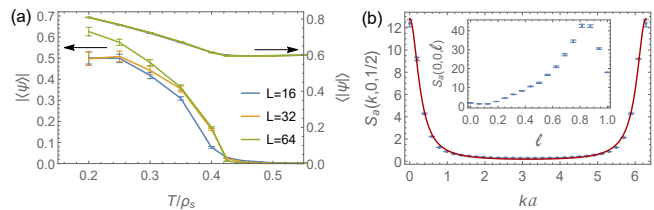


FIG. 3. (a) The average superconducting order parameter and its average magnitude for a system of size  $L \times L \times 16$  with  $V^2 = 0.035$ ,  $\xi_{\text{dis}} = 2$  and  $\tilde{V}^2 = 0$ . (b) A Lorentzian fit of  $S_a(k,0,1/2)$  for a  $32^3$  system with similar parameters at  $T = 0.4$ . The inset depicts the  $l$  dependence of  $S_a$ .

ple, reducing  $\xi_{\text{dis}}$  from 2 to 0.2 while keeping all other parameters fixed causes  $S_a$  to shrink by a factor of approximately 4 (concomitantly,  $T_c$  increases by only 10%). Hence, to maintain the experimentally observed 2:1 ratio between  $S_a$  of the two systems [40] we need to increase the variance of the potential by tenfold when we eliminate its spatial correlations. This change also leads to a similar temperature dependence of  $S_a$  for the two systems, as shown by Fig. 1. Such behavior aligns with the experimental findings [40].

We extract the in-plane CDW correlation length by fitting  $S_a(k,0,1/2)$  to a Lorentzian  $c + b/(k^2 + \xi_{\text{CDW}}^{-2}) + b/((2\pi - k)^2 + \xi_{\text{CDW}}^{-2})$ , as exemplified in Fig. 3b. The results, presented in Fig. 2 show that, similar to the amplitude of the structure factor, the CDW correlation length retains its temperature dependence upon reducing  $\xi_{\text{dis}}$  and rescaling of  $V^2$ . It remains essentially constant up to  $T_c$  and then diminishes with increasing temperature. Nevertheless, we find that complete disordering of the chain layer reduces  $\xi_{\text{CDW}}$  by one third, which is significantly larger than the observed reduction [40].

To conclude this section, we note that  $S_a$  exhibits an asymmetric peak around  $l = 0.8$ , as shown in the inset of Fig. 3b. This arises from the form factor in Eq. (6). We have checked that  $S_a$  presents the same qualitative behavior outlined above also at  $l = 0.8$  or when only the diagonal terms ( $\mu = \mu'$ ) are kept in Eq. (6).

## B. Gaussian disorder on the $\text{CuO}_2$ planes

Next, we fix  $\xi_{\text{dis}} = 2$ ,  $V^2 = 0.035$  for the potential in the chain layers and consider the effects of local Gaussian disorder on the  $\text{CuO}_2$  planes. Figure 4 depicts the temperature evolution of the structure factor for various values of the in-plane disorder variance  $\tilde{V}^2$ . Evidently, when the disorder is not too strong  $S_a$  exhibits a maximum, which coincides (within numerical errors) with  $T_c$ . The maximum moves to lower temperatures and becomes less pronounced as  $\tilde{V}^2$  increases, until it eventually disappears. Instead, we find at  $T_c$  a break in the slope of  $S_a$  or, for the most disordered systems, a smooth decrease of the structure factor with temperature.

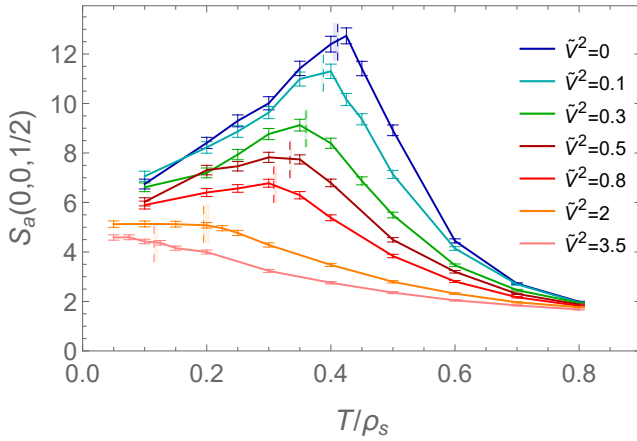


FIG. 4. The temperature dependence of the peak amplitude  $S_a(0,0,1/2)$  for  $32^3$  systems with  $V^2 = 0.035$ ,  $\xi_{\text{dis}} = 2$  and various values of  $\tilde{V}^2$ . For each case the corresponding  $T_c$  is denoted by a dashed vertical line.

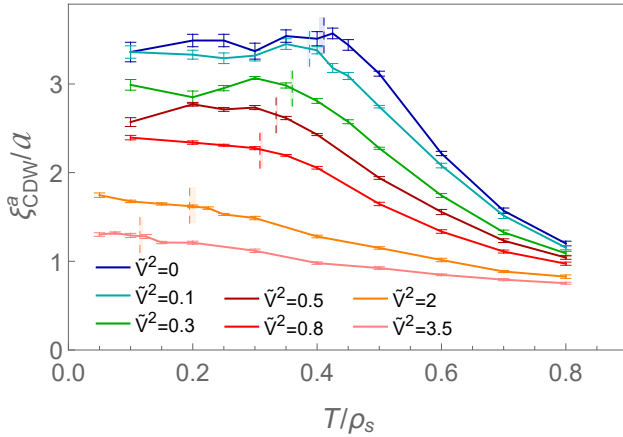


FIG. 5. The temperature dependence of the CDW correlation length for the same systems as in Fig. 4.

Insights into the reasons behind this behavior of  $S_a$  can be gleaned from the CDW correlation length, as presented in Fig. 5, and the average (squared) magnitude of the CDW field  $\Phi^a$ , as shown in Fig. 6. For weak disorder the correlation length increases with decreasing temperature and then remains approximately constant below  $T_c$ . At the same time, the magnitude of the CDW order parameter is approximately constant above  $T_c$  and then decreases below  $T_c$ . Hence, the increase of the CDW structure factor above  $T_c$  is due to the establishment of longer range CDW coherence while its decrease below  $T_c$  is driven by the decrease in the average magnitude of the CDW order parameter due to its competition with superconductivity. For strong disorder the local magnitude of the CDW order is enhanced by the interaction with the potential on the  $\text{CuO}_2$  layers, but its correlation length is smaller. Both change more gradually than in the cleaner systems, leading to a smoother evolution of the structure factor. The overall decrease in the magnitude of the

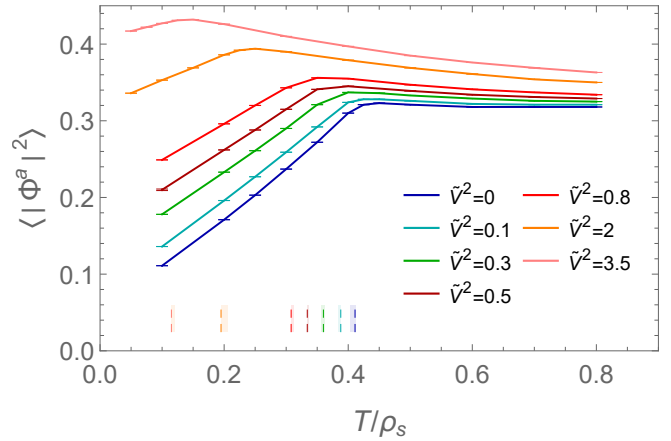


FIG. 6. The temperature evolution of the squared magnitude of the CDW field  $\Phi^a$  for the same systems as in Fig. 4.

structure factor with increasing disorder is largely due to the reduction in the correlation length.

We have already noted that gauge invariance precludes direct linear coupling between the disorder and the superconducting order. Consequently, the reduction in  $T_c$  with increasing  $\tilde{V}^2$  can result from two effects. First, the suppression of the magnitude of the superconducting order by the competition with the locally enhanced CDW. Secondly, by phase disordering due to the same competition with the disordered CDW fields. Figure 6 together with the constraint Eq. (1) show that in the weak disorder regime the superconducting amplitude changes relative little above  $T_c$  as a function of the disorder strength. Hence, the reduction of  $T_c$  in this regime is mostly driven by phase fluctuations. For strong disorder the superconducting amplitude is more significantly suppressed and this effect also contributes to the decrease in  $T_c$ .

#### IV. LARGE $N$ ANALYSIS

Analytical progress in analyzing the problem can be made by enlarging the number of real components of the vector of order parameters from 6 to  $N \gg 1$ . The superconducting order is described by the real fields  $n_{j\mu}^\alpha(\mathbf{r})$ , with  $\alpha = 1, \dots, N/3$ , while the CDW fields  $\Phi^{a,b}$  are described by  $n_{j\mu}^\alpha(\mathbf{r})$ , with  $\alpha = N/3 + 1, \dots, 2N/3$ , and  $\alpha = 2N/3 + 1, \dots, N$ , respectively. The Hamiltonian becomes

$$\begin{aligned}
 H = & \sum_{\alpha=1}^N \sum_{j\mu} \int d^2r \left[ \frac{\lambda_\alpha}{2} (\nabla n_{j\mu}^\alpha)^2 + \frac{g_\alpha}{2} (n_{j\mu}^\alpha)^2 + \tilde{\mathcal{V}}_{j\mu}^\alpha n_{j\mu}^\alpha \right] \\
 & + \sum_{\alpha=1}^N \sum_j \int d^2r \left[ \tilde{W}_\alpha n_{j0}^\alpha n_{j1}^\alpha + W_\alpha n_{j1}^\alpha n_{j+1,0}^\alpha \right. \\
 & \left. + \mathcal{V}_j^\alpha (n_{j1}^\alpha + n_{j+1,0}^\alpha) \right], \quad (7)
 \end{aligned}$$

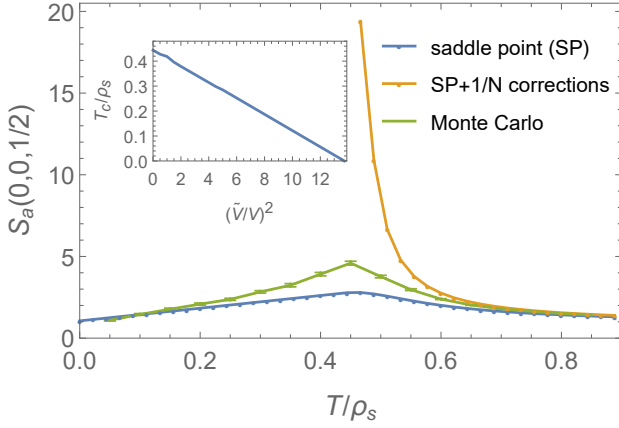


FIG. 7. Comparing the saddle-point results, with and without  $1/N$ -corrections, to Monte Carlo calculations of  $S_a(0,0,1/2)$  for a  $32^2 \times 16$  systems with Gaussian  $V^2 = 0.1$  chain-layer potential and  $\tilde{V} = 0$ . The inset depicts the saddle-point  $T_c$  as a function of  $\tilde{V}^2/V^2$ .

where we have already set  $\rho_s = 1$ . In order to be able to carry out the disorder averaging we assume that *both* the chain layer potentials  $\mathcal{V}_j^\alpha$  and the  $\text{CuO}_2$  layer potentials  $\tilde{\mathcal{V}}_{j\mu}^\alpha$  are independent local random Gaussian fields with respective variances  $V_\alpha^2/N$  and  $\tilde{V}_\alpha^2/N$ , scaled to ensure  $N$ -independent results as  $N \rightarrow \infty$ . In Eq. (7),  $g_\alpha = 0$ ,  $W_\alpha = -J$ ,  $\tilde{W}_\alpha = -\tilde{J}$ ,  $V_\alpha = 0$  and  $\tilde{V}_\alpha = 0$  for the superconducting components, while for the CDW components  $g_\alpha = g$ ,  $W_\alpha = U$ ,  $\tilde{W}_\alpha = \tilde{U}$ ,  $V_\alpha = V$  and  $\tilde{V}_\alpha = \tilde{V}$ .

Taking into account the constraints of the NLSM, the partition function reads

$$Z = e^{-N\beta F} = \int \mathcal{D}n \prod_{j\mu} \delta \left[ \sum_{\alpha} (n_{j\mu}^{\alpha})^2 - 1 \right] e^{-S}, \quad (8)$$

with

$$S = N\beta H + \int d^2r d^2r' \sum_{\alpha\beta jj'\mu\mu'} K_{jj'\mu\mu'}^{\alpha\beta}(\mathbf{r}, \mathbf{r}') n_{j\mu}^{\alpha}(\mathbf{r}) n_{j'\mu'}^{\beta}(\mathbf{r}') \quad (9)$$

where the scaling  $N\beta$  is used to facilitate a sensible large- $N$  limit. The source term  $K$  is introduced for the purpose of evaluating the Green's functions via

$$\mathcal{G}_{jj'\mu\mu'}^{\alpha\beta}(\mathbf{r}, \mathbf{r}') \equiv \overline{\langle n_{j\mu}^{\alpha}(\mathbf{r}) n_{j'\mu'}^{\beta}(\mathbf{r}') \rangle} = \left. \frac{\delta N\beta \bar{F}}{\delta K_{jj'\mu\mu'}^{\alpha\beta}(\mathbf{r}, \mathbf{r}')} \right|_{K=0}. \quad (10)$$

To calculate  $\bar{F}$  we consider  $R$  replicas of the model and

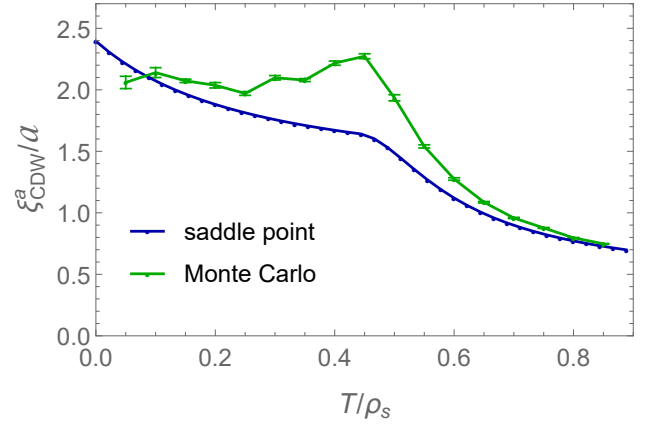


FIG. 8. The CDW correlation length for the system presented in Fig. 7, calculated using the saddle point approximation and Monte Carlo simulations.

use the replica trick  $\bar{F} = \lim_{R \rightarrow 0} F_R/R$ , where

$$e^{-N\beta F_R} = \int \mathcal{D}n \mathcal{D}\mathcal{V} \mathcal{D}\tilde{\mathcal{V}} \mathcal{D}\sigma \exp \left\{ - \sum_{a=1}^R S(n_{j\mu}^{\alpha a}) + \int d^2r \left[ i \frac{N\beta}{2} \sum_{j\mu} \sum_{a=1}^R \sigma_{j\mu}^a \left( 1 - \sum_{\alpha} (n_{j\mu}^{\alpha a})^2 \right) - N \sum_{j\alpha} \left( \frac{|\mathcal{V}_j^{\alpha}|^2}{2V_\alpha^2} + \sum_{\mu} \frac{|\tilde{\mathcal{V}}_{j\mu}^{\alpha}|^2}{2\tilde{V}_\alpha^2} \right) \right] \right\}. \quad (11)$$

Here,  $a$  is the replica index and we have incorporated the constraints by an integral over the Lagrange multiplier fields  $\sigma_{j\mu}^a$ . Carrying out the disorder integrals we find  $e^{-N\beta F_R} = \int \mathcal{D}n \mathcal{D}\sigma e^{-\tilde{S}_R}$ , given in terms of

$$\tilde{S}_R = \frac{1}{2} \int d^2r d^2r' \sum_{\alpha\beta jj'ab} [ n_{j0}^{\alpha a}(\mathbf{r}) n_{j'1}^{\alpha a}(\mathbf{r}') ] \times \left[ \left( \hat{G}^{-1} + 2\hat{K} \right)_{jj'}^{\alpha\beta ab}(\mathbf{r}, \mathbf{r}') \right] \begin{bmatrix} n_{j'0}^{\beta b}(\mathbf{r}') \\ n_{j'1}^{\beta b}(\mathbf{r}') \end{bmatrix} - i \frac{N\beta}{2} \int d^2r \sum_{j\mu a} \sigma_{j\mu}^a, \quad (12)$$

where a hat denotes a  $2 \times 2$  matrix with indices  $\mu, \mu'$ . We also define  $\hat{K}_{\mu\mu'jj'}^{\alpha\beta ab}(\mathbf{r}, \mathbf{r}') = \delta_{ab} K_{\mu\mu'jj'}^{\alpha\beta}(\mathbf{r}, \mathbf{r}')$ , and

$$\left( \hat{G}^{-1} \right)_{jj'}^{\alpha\beta ab}(\mathbf{r}, \mathbf{r}') = N\beta \left[ \delta_{ab} \hat{L}_{jj'}^{\alpha a} - \hat{M}_{jj'}^{\alpha} \right] \delta_{\alpha\beta} \delta(\mathbf{r} - \mathbf{r}'). \quad (13)$$

The latter contains the interaction and disorder parts

$$\hat{L}_{jj'}^{\alpha a} = \begin{bmatrix} \mathcal{L}_{jj'0}^{\alpha a} & \tilde{W}_\alpha \delta_{j'j} + W_\alpha \delta_{j',j-1} \\ \tilde{W}_\alpha \delta_{j'j} + W_\alpha \delta_{j',j+1} & \mathcal{L}_{jj'1}^{\alpha a} \end{bmatrix} \quad (14)$$

$$\hat{M}_{jj'}^{\alpha} = \beta V_\alpha^2 \begin{bmatrix} (1 + v_\alpha^2) \delta_{jj'} & \delta_{j',j-1} \\ \delta_{j',j+1} & (1 + v_\alpha^2) \delta_{jj'} \end{bmatrix}, \quad (15)$$

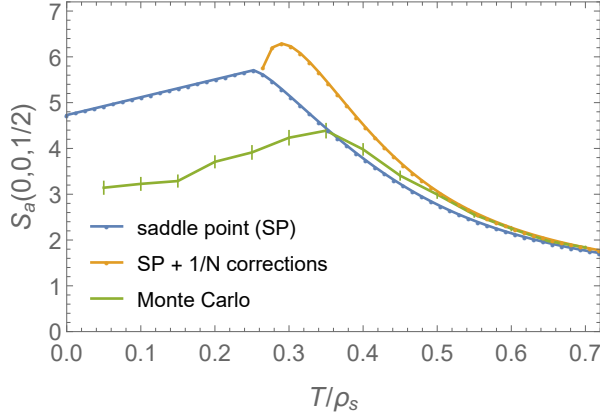


FIG. 9. Comparing the saddle-point results, with and without  $1/N$ -corrections, to Monte Carlo calculations of  $S_a(0,0,1/2)$  for a  $32^2 \times 16$  systems with Gaussian  $V^2 = 0.1$  chain-layer potential and Gaussian  $\tilde{V}^2 = 0.6$  disorder on the  $\text{CuO}_2$  planes.

involving

$$\mathcal{L}_{jj'\mu}^{\alpha a} = [-\lambda_\alpha \nabla^2 + g_\alpha + i\sigma_{j\mu}^a(\mathbf{r})] \delta_{jj'}, \quad (16)$$

$$v_\alpha^2 = \tilde{V}_\alpha^2/V_\alpha^2. \quad (17)$$

Next, we integrate out the  $n$  fields. To allow for spontaneous symmetry breaking in the superconducting channel, which amounts to  $(n^1, n^2) = O(1)$ , we denote  $\psi_{j\mu}^a = n_{j\mu}^{1a} + in_{j\mu}^{2a}$  and avoid integrating over it (consequently, henceforth,  $\alpha = 3, \dots, N$ ). The result is

$$e^{-N\beta F_R} = \int \mathcal{D}\sigma^a \mathcal{D}\psi^a e^{-S_R}, \quad (18)$$

where

$$S_R = \frac{1}{2} \text{Tr} \ln(G^{-1} + 2K) + \frac{N\beta}{2} \int d^2r \left\{ \sum_{j\mu a} [|\nabla \psi_{j\mu}^a|^2 + i\sigma_{j\mu}^a (|\psi_{j\mu}^a|^2 - 1)] - \sum_{ja} \left( \tilde{J} \psi_{j0}^{a*} \psi_{j1}^a + J \psi_{j1}^{a*} \psi_{j+1,0}^a + \text{c.c.} \right) \right\}. \quad (19)$$

### A. Saddle-point approximation

The integrals over  $\sigma_{j\mu}^a$  and  $\psi_{j\mu}^a$  in Eq. (18) are to be calculated using a saddle-point approximation, which is justified in the limit  $N \rightarrow \infty$ . Within this approximation,  $N\beta F_R = S_R$ , where  $S_R$  is evaluated using its saddle-point configurations. To evaluate the Green's function  $\mathcal{G}_{\mu\mu'jj'}^{\alpha\beta}(\mathbf{r}, \mathbf{r}')$  it is therefore necessary to know  $S_R$  to first order in  $K$ . One can check that it is sufficient for this purpose to use the saddle point configurations of  $S_R^0 \equiv S_R|_{K=0}$ , as this entails only  $O(K^2)$  corrections. Varying

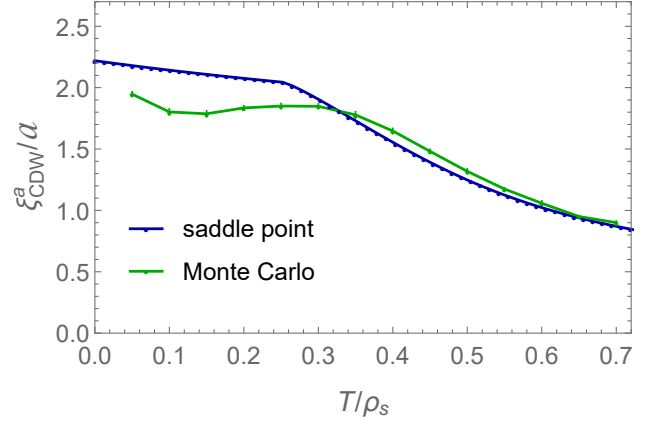


FIG. 10. The CDW correlation length for the system presented in Fig. 9, calculated using the saddle point approximation and Monte Carlo simulations.

$S_R^0$  with respect to  $\sigma_{j\mu}^a(\mathbf{r})$  and  $\psi_{j\mu}^{a*}(\mathbf{r})$  yields the saddle point equations

$$\sum_{\alpha} G_{jj\mu\mu}^{\alpha\alpha a a}(\mathbf{r}, \mathbf{r}) = 1 - |\psi_{j\mu}^a|^2, \quad (20)$$

$$(-\nabla^2 + i\sigma_{\mu j}^a) \psi_{\mu j}^a = \tilde{J} (\delta_{\mu 0} \psi_{1j}^a + \delta_{\mu 1} \psi_{0j}^a) + J (\delta_{\mu 0} \psi_{1j-1}^a + \delta_{\mu 1} \psi_{0j+1}^a). \quad (21)$$

Since  $G^{-1}$  is diagonal in  $\alpha, \beta$  and symmetric in  $a, b, \mathbf{r}, \mathbf{r}'$ , and under exchange of both  $j, j'$  and  $\mu, \mu'$  so is  $G_{jj'\mu\mu'}^{\alpha\beta ab} = \delta_{\alpha\beta} G_{jj'\mu\mu'}^{\alpha ab}$ . Thus, it follows from Eqs. (10) and (19) that

$$\hat{G}_{jj'}^{\alpha\beta}(\mathbf{r}, \mathbf{r}') \equiv \delta_{\alpha\beta} \hat{G}_{jj'}^{\alpha}(\mathbf{r}, \mathbf{r}') = \delta_{\alpha\beta} \lim_{m \rightarrow 0} \frac{1}{m} \sum_a \hat{G}_{jj'}^{\alpha a a}(\mathbf{r}, \mathbf{r}'), \quad (22)$$

where  $\hat{G}$  is evaluated using the saddle point solutions.

We will calculate the  $2 \times 2$  correlation matrix  $\hat{G}_{jj'}^{\alpha ab}$  by assuming a replica-symmetric solution of the saddle-point equations, which is also independent of  $j, \mu$  and  $\mathbf{r}$ , *i.e.*,  $\psi_{\mu j}^a = \psi$ ,  $\sigma_{\mu j}^a(\mathbf{r}) = -i\sigma$ . Under this assumption the interaction part, Eq. (14), is also replica symmetric  $\hat{L}_{jj'}^{\alpha a} = \hat{L}_{jj'}^{\alpha}$  and  $\hat{G}_{jj'}^{\alpha ab}$  is determined from

$$N\beta \sum_{cl} \int d^2\tilde{r} [\delta_{ac} \hat{L}_{jl}^{\alpha} - \hat{M}_{jl}^{\alpha}] \delta(\mathbf{r} - \tilde{\mathbf{r}}) \hat{G}_{l j'}^{\alpha cb}(\tilde{\mathbf{r}}, \mathbf{r}') = \hat{I} \delta_{jj'} \delta_{ab} \delta(\mathbf{r} - \mathbf{r}'). \quad (23)$$

Expanding

$$\hat{G}_{jj'}^{\alpha ab}(\mathbf{r}, \mathbf{r}') = \frac{2}{L^2 L_z} \sum_{\mathbf{k}, k_z} \hat{G}^{\alpha ab}(k) e^{i[\mathbf{k} \cdot (\mathbf{r} - \mathbf{r}') + k_z(j - j')]}, \quad (24)$$

we find that Eq. (23) is solved by  $\hat{G}^{\alpha ab}(k) = \hat{A}^{\alpha}(k) \delta_{ab} + \hat{B}^{\alpha}(k)$ , where, henceforth,  $k \equiv (\mathbf{k}, k_z)$ . This leads by Eq. (22) to the correlation matrix

$$\hat{G}^{\alpha}(k) = \hat{A}^{\alpha}(k) + \hat{B}^{\alpha}(k), \quad (25)$$

with

$$\hat{A}^\alpha(k) = \frac{1}{N\beta} \frac{1}{\epsilon_\alpha^2(\mathbf{k}) - \epsilon_{\alpha\perp}^2(k_z)} \times \begin{bmatrix} \epsilon_\alpha(\mathbf{k}) & -\tilde{W}_\alpha - W_\alpha e^{-ik_z} \\ -\tilde{W}_\alpha - W_\alpha e^{ik_z} & \epsilon_\alpha(\mathbf{k}) \end{bmatrix}, \quad (26)$$

and where the components of  $\hat{B}_\alpha$  are given by

$$\begin{aligned} (B^\alpha)_{00}(k) &= (B^\alpha)_{11}(k) \\ &= \frac{1}{N} \frac{V_\alpha^2}{[\epsilon_\alpha(\mathbf{k})^2 - \epsilon_{\alpha\perp}^2(k_z)]^2} \\ &\quad \times \left\{ (1 + v_\alpha^2) [\epsilon_\alpha(\mathbf{k})^2 + \epsilon_{\alpha\perp}^2(k_z)] \right. \\ &\quad \left. - 2\epsilon_\alpha(\mathbf{k}) (W_\alpha + \tilde{W}_\alpha \cos k_z) \right\}, \quad (27) \end{aligned}$$

$$\begin{aligned} (B^\alpha)_{01}(k) &= (B^\alpha)_{10}^*(k) \\ &= \frac{1}{N} \frac{V_\alpha^2 e^{-ik_z}}{[\epsilon_\alpha(\mathbf{k})^2 - \epsilon_{\alpha\perp}^2(k_z)]^2} \\ &\quad \times \left\{ [W_\alpha - \epsilon_\alpha(\mathbf{k}) + \tilde{W}_\alpha e^{ik_z}]^2 \right. \\ &\quad \left. - 2v_\alpha^2 \epsilon_\alpha(\mathbf{k}) (W_\alpha + \tilde{W}_\alpha e^{ik_z}) \right\}. \quad (28) \end{aligned}$$

Here,

$$\epsilon_\alpha(\mathbf{k}) = \begin{cases} \lambda_\alpha(k_x^2 + k_y^2) + g_\alpha + \sigma & \text{continuum} \\ 2\lambda_\alpha(2 - \cos k_x - \cos k_y) + g_\alpha + \sigma & \text{lattice} \end{cases}, \quad (29)$$

$$\epsilon_{\alpha\perp}(k_z) = \sqrt{W_\alpha^2 + \tilde{W}_\alpha^2 + 2W_\alpha\tilde{W}_\alpha \cos k_z}. \quad (30)$$

Under our ansatz, the saddle point equation (21) becomes  $\psi(\sigma - J - \tilde{J}) = 0$ . It is either solved by  $\psi = 0$  and  $\sigma$  that is then determined by Eq. (20), or by  $\sigma = J + \tilde{J}$  and  $\psi$  that is given by Eq. (20). The first solution holds at high temperatures. When  $T$  decreases,  $\sigma$  decreases with it, reaching  $J + \tilde{J}$  at  $T = T_c$  and sticking at this value for lower temperatures where  $\psi \neq 0$ . As the inset of Fig. 7 shows, we find that the saddle point estimate of  $T_c$  vanishes linearly with  $\tilde{V}^2/V^2$ .

In Figs. 7-10 we compare the saddle point predictions for the temperature evolution of the structure factor and the CDW correlation length with Monte Carlo results for the  $N = 6$  model. To this end, we note that  $S_a(\mathbf{k}, k_z) = 4G_{00}^\alpha(\mathbf{k}, k_z) + 4\text{Re}[G_{01}^\alpha(\mathbf{k}, k_z) \exp(ik_z/3)]$ , where  $\hat{G}^\alpha$  is the correlation matrix for one of the CDW components. Furthermore, the scaling of  $T$  and  $V^2$ , used in defining the large- $N$  model, implies that they correspond to  $T/N$  and  $V^2/N$  in the Monte Carlo simulations. Our results show that for the case  $\tilde{V}^2 = 0$ , the saddle point approximation yields a reasonable estimate for  $T_c$  as well as for the high and low temperature behavior of  $S_a$ . However, it underestimates  $S_a$  in the vicinity of  $T_c$ . The same statements hold for  $\xi_{\text{CDW}}$ . The picture changes for  $\tilde{V}^2 > 0$ , where the saddle point approximation underestimates  $T_c$  and overestimates both  $S_a$  and  $\xi_{\text{CDW}}$  at low temperatures.

## B. $1/N$ corrections

Next, we consider  $1/N$  corrections to the saddle-point [43]. We do so for the symmetric phase  $\psi = 0$  where the part of the action involving  $\psi$  is identical to that of the other components with  $\alpha = 3, \dots, N/3$ , and we include it in the integration over  $n^\alpha$ . To proceed we expand  $\sigma_{j\mu}^\alpha = -i\sigma + \eta_{j\mu}^\alpha$  and plug it into Eq. (19). The result is

$$S_R = \frac{1}{2} \text{Tr} \ln(G^{-1} + i\Lambda + 2K) - i \frac{N\beta}{2} \int d^2r \sum_{a\mu j} \eta_{j\mu}^a, \quad (31)$$

where  $G$  is evaluated at the saddle point  $-i\sigma$  and

$$\Lambda_{jj'\mu\mu'}^{\alpha\beta ab}(\mathbf{r}, \mathbf{r}') = N\beta \eta_{j\mu}^\alpha(\mathbf{r}) \delta_{\alpha\beta} \delta_{ab} \delta_{jj'} \delta_{\mu\mu'} \delta(\mathbf{r} - \mathbf{r}'). \quad (32)$$

Consequently, using the symmetry properties of  $G$  and the fact that it satisfies the saddle point equation (20) we obtain that apart from a  $K$ -independent piece

$$N\beta F_R = \text{Tr}(GK) - \ln \left[ \int \mathcal{D}\lambda e^{-S_0(\Lambda) - S_{\text{int}}(\Lambda)} \right], \quad (33)$$

where

$$S_0 = \frac{1}{2} \sum_{ab} \sum_{\mu\mu'} \int \frac{d^3k}{(2\pi)^3} \eta_\mu^a(k) \chi^{-1ab}_{\mu\mu'}(k) \eta_{\mu'}^b(-k), \quad (34)$$

with

$$\chi^{-1ab}_{\mu\mu'}(k) = \frac{(N\beta)^2}{2} \int \frac{d^3q}{(2\pi)^3} \sum_\alpha G_{\mu\mu'}^{\alpha ab}(q) G_{\mu'\mu}^{\alpha ba}(q+k). \quad (35)$$

To linear order in  $K$

$$S_{\text{int}} = \text{Tr} \left[ \sum_{n=1}^{\infty} (-i)^n (G\Lambda)^n GK - \frac{1}{2} \sum_{n=3}^{\infty} \frac{(-i)^n}{n} (G\Lambda)^n \right]. \quad (36)$$

The linked cluster theorem implies

$$\ln \left[ \int \mathcal{D}\lambda e^{-S_0 - S_{\text{int}}} \right] = \ln \left[ \int \mathcal{D}\lambda e^{-S_0} \right] + \langle e^{-S_{\text{int}}} \rangle_{\text{conn}} - 1, \quad (37)$$

where  $\langle A \rangle_{\text{conn}}$  is the sum over all connected diagrams generated by averaging  $A$  with respect to  $S_0$ . We focus on the diagrams of the type presented in Fig. 11, which provide a  $1/N$  correction to the correlation matrix. This conclusion is based on the fact that both  $\hat{G}^\alpha(k)$  and  $\hat{\chi}^\alpha(k)$  scale as  $1/N$ , while each vertex at the end of a  $\chi$  line contributes a factor  $N$ . Hence, the blocks  $\hat{X}^\alpha(k)$  and  $\hat{Y}^\alpha(k)$  that appear in the self energy are both of order  $1/N$  ( $\hat{Y}$  contains an additional factor of  $N$  coming from the sum over the fields in the loop). Explicitly,

$$\hat{X}^\alpha(k) = -\hat{G}^\alpha(k) \hat{F}^\alpha(k), \quad (38)$$

$$\hat{Y}^\alpha(k) = \frac{1}{2} \hat{G}^\alpha(k) \hat{\Gamma}, \quad (39)$$

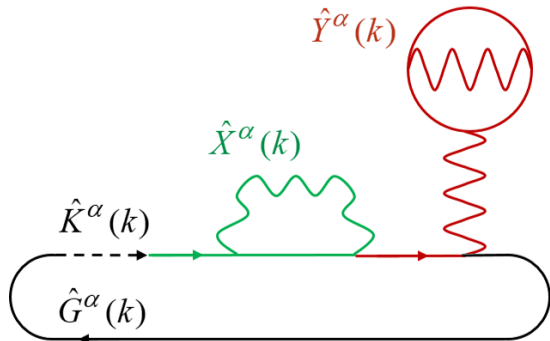


FIG. 11. A typical diagram that contributes to the  $1/N$  correction. A broken line represents  $\hat{K}^\alpha(k)$ , a solid line  $\hat{G}^\alpha$  and a wavy line  $\hat{\chi}(k)$ . The full correction is the sum over such diagrams with all possible sequences of  $\hat{X}^\alpha(k)$  and  $\hat{Y}^\alpha(k)$  blocks.

where

$$F_{\mu\mu'}^\alpha(k) = (N\beta)^2 \int \frac{d^3q}{(2\pi)^3} G_{\mu\mu'}^\alpha(k+q) \chi_{\mu'\mu}(q), \quad (40)$$

$$\Gamma_{\mu\mu'} = \delta_{\mu\mu'} (N\beta)^2 \sum_{\nu_1\nu_2\nu_3} \sum_{\alpha} \int \frac{d^3q}{(2\pi)^3} G_{\nu_1\nu_3}^\alpha(q) \times F_{\nu_3\nu_2}^\alpha(q) G_{\nu_2\nu_1}^\alpha(q) \chi_{\nu_1\mu}(0). \quad (41)$$

In the above we have suppressed the replica indices on the various quantities, since to obtain a result that is proportional to  $R$  they must all equal each other.

Summing over the diagrams [including the zeroth order one  $\text{Tr}(GK)$ ], and using Eq. (10), we arrive at

$$\hat{G}^{\alpha\beta}(k) = \delta_{\alpha\beta} \left[ \hat{1} - \hat{X}^\alpha(k) - \hat{Y}^\alpha(k) \right]^{-1} \hat{G}^\alpha(k), \quad (42)$$

or

$$\hat{G}^{\alpha\beta}(k)^{-1} = \delta_{\alpha\beta} \left[ \hat{G}^\alpha(k)^{-1} + \hat{F}^\alpha(k) - \frac{1}{2} \hat{\Gamma} \right]. \quad (43)$$

Figure 7 illustrates the impact of including the  $1/N$  corrections in the case  $\tilde{V} = 0$ . Evidently, while the corrections align the analytical results more closely with the Monte Carlo simulations at high temperatures, they significantly overestimate the CDW structure factor peak around  $T_c$ . In the system with  $\tilde{V} > 0$ , depicted in Fig. 9, the corrections shift the maximum of  $S_a(0,0,1/2)$  to a somewhat higher temperature, bringing it closer to the temperature at which the Monte Carlo results attain a maximum. Although the agreement with Monte Carlo

simulations also improves at high temperatures, the analytical results still overestimate the numerical outcomes at intermediate temperatures, similar to the  $\tilde{V} = 0$  case.

## V. CONCLUSIONS

One of the goals of the present study was to explore the extent to which the observations of Achkar et al. [40] can be explained from the perspective of competing superconducting and CDW orders and their coupling to the chain-layer potential. We have shown that one of these findings, namely, that the disordering of the oxygen ortho structure cuts the amplitude of the CDW structure factor in half but leaves its temperature dependence unchanged, is reproduced to a good approximation by the model. We have found that eliminating the potential correlations in the chain-layer reduces the average local amplitude of CDW order by only a few percents. Hence, the large reduction in the model's structure factor arises from the degradation of the CDW phase correlations. This fact is also apparent in the decrease of the CDW correlation length. Here, however, the model departs from the experiment where the changes in correlation length were relatively minor, especially below  $T_c$ .

Whereas disorder on the chain layers does not preclude the onset of long-range CDW order (with  $l = 1$ ) [39], the same is not true for disorder on the  $\text{CuO}_2$  planes. Elucidating the effects of the latter on the CDW correlations at  $l = 1/2$  constituted the second goal of our work. We have shown that, for sufficiently weak disorder, the structure factor attains a maximum at  $T_c$ , which by itself diminishes with increasing disorder strength, predominantly due to degradation of the superconducting phase coherence. The structure factor peak at  $T_c$  arises from enhanced CDW phase correlations as the temperature is lowered toward  $T_c$ , coupled with a reduction in the magnitude of the CDW order parameter once superconductivity is established below  $T_c$ . As disorder is increased, the overall size of the CDW structure factor decreases. This happens despite an increase in the magnitude of the local CDW order due to its nucleation by the planar disorder, a fact which also contributes to the reduction of  $T_c$ . At the same time however, the disorder disrupts the onset of CDW phase coherence, causing the CDW correlation length, and with it the structure factor, to decrease. Consequently, the temperature dependence of the structure factor becomes more monotonic; the peak at  $T_c$  first transitions into a change in slope, then eventually disappears altogether. It would be interesting to contrast these expected behaviors with experiments where the level of disorder can be controlled by sample irradiation.

## ACKNOWLEDGEMENTS

We thank A. Carrington and S. Hayden for useful discussions.

- [1] J. M. Tranquada, B. J. Sternlieb, J. D. Axe, Y. Nakamura, and S. Uchida, Evidence for stripe correlations of spins and holes in copper oxide superconductors, *Nature (London)* **375**, 561 (1995).
- [2] M. v. Zimmermann, A. Vigliante, T. Niemöller, N. Ichikawa, T. Frello, J. Madsen, P. Wochner, S. Uchida, N. H. Andersen, J. M. Tranquada, D. Gibbs, and J. R. Schneider, Hard-X-ray diffraction study of charge stripe order in  $\text{La}_{1.48}\text{Nd}_{0.4}\text{Sr}_{0.12}\text{CuO}_4$ , *Europhys. Lett.* **41**, 629 (1998).
- [3] A. W. Hunt, P. M. Singer, K. R. Thurber, and T. Imai,  $^{63}\text{Cu}$  NQR measurement of stripe order parameter in  $\text{La}_{2-x}\text{Sr}_x\text{CuO}_4$ , *Phys. Rev. Lett.* **82**, 4300 (1999).
- [4] M. Hücker, M. v. Zimmermann, G. D. Gu, Z. J. Xu, J. S. Wen, G. Xu, H. J. Kang, A. Zheludev, and J. M. Tranquada, Stripe order in superconducting  $\text{La}_{2-x}\text{Ba}_x\text{CuO}_4$  ( $0.095 \leq x \leq 0.155$ ), *Phys. Rev. B* **83**, 104506 (2011).
- [5] G. Ghiringhelli, M. Le Tacon, M. Minola, S. Blanco-Canosa, C. Mazzoli, N. B. Brookes, G. M. De Luca, A. Frano, D. G. Hawthorn, F. He, T. Loew, M. Moretti Sala, D. C. Peets, M. Salluzzo, E. Schierle, R. Sutarto, G. A. Sawatzky, E. Weschke, B. Keimer, and L. Braicovich, Long-range incommensurate charge fluctuations in  $(\text{Y,Nd})\text{Ba}_2\text{Cu}_3\text{O}_{6+x}$ , *Science* **337**, 821 (2012).
- [6] J. Chang, E. Blackburn, A. T. Holmes, N. B. Christensen, J. Larsen, J. Mesot, R. Liang, D. A. Bonn, W. N. Hardy, A. Watenphul, M. v. Zimmermann, E. M. Forgan, and S. M. Hayden, Direct observation of competition between superconductivity and charge density wave order in  $\text{YBa}_2\text{Cu}_3\text{O}_{6.67}$ , *Nat. Phys.* **8**, 871 (2012).
- [7] A. J. Achkar, R. Sutarto, X. Mao, F. He, A. Frano, S. Blanco-Canosa, M. Le Tacon, G. Ghiringhelli, L. Braicovich, M. Minola, M. Moretti Sala, C. Mazzoli, R. Liang, D. A. Bonn, W. N. Hardy, B. Keimer, G. A. Sawatzky, and D. G. Hawthorn, Distinct charge orders in the planes and chains of ortho-III-ordered  $\text{YBa}_2\text{Cu}_3\text{O}_{6+\delta}$  superconductors identified by resonant elastic x-ray scattering, *Phys. Rev. Lett.* **109**, 167001 (2012).
- [8] E. Blackburn, J. Chang, M. Hücker, A. T. Holmes, N. B. Christensen, R. Liang, D. A. Bonn, W. N. Hardy, U. Rütt, O. Gutowski, M. v. Zimmermann, E. M. Forgan, and S. M. Hayden, X-ray diffraction observations of a charge-density-wave order in superconducting ortho-II  $\text{YBa}_2\text{Cu}_3\text{O}_{6.54}$  single crystals in zero magnetic field, *Phys. Rev. Lett.* **110**, 137004 (2013).
- [9] R. Comin, A. Frano, M. M. Yee, Y. Yoshida, H. Eisaki, E. Schierle, E. Weschke, R. Sutarto, F. He, A. Soumyanarayanan, Yang He, M. Le Tacon, I. S. Elfimov, J. E. Hoffman, G. A. Sawatzky, B. Keimer, and A. Damascelli, Charge order driven by Fermi-arc instability in  $\text{Bi}_2\text{Sr}_{2-x}\text{La}_x\text{CuO}_{6+\delta}$ , *Science* **343**, 390 (2014).
- [10] E. H. da Silva Neto, P. Aynajian, A. Frano, R. Comin, E. Schierle, E. Weschke, A. Gyenis, J. Wen, J. Schneeloch, Z. Xu, S. Ono, G. Gu, M. Le Tacon, and A. Yazdani, Ubiquitous interplay between charge ordering and high-temperature superconductivity in cuprates, *Science* **343**, 393 (2014).
- [11] M. Le Tacon, A. Bosak, S. M. Souliou, G. Dellea, T. Loew, R. Heid, K.-P. Bohnen, G. Ghiringhelli, M. Krisch, and B. Keimer, Inelastic x-ray scattering in  $\text{YBa}_2\text{Cu}_3\text{O}_{6.6}$  reveals giant phonon anomalies and elastic central peak due to charge-density-wave formation, *Nat. Phys.* **10**, 52 (2014).
- [12] M. Hücker, N. B. Christensen, A. T. Holmes, E. Blackburn, E. M. Forgan, R. Liang, D. A. Bonn, W. N. Hardy, O. Gutowski, M. v. Zimmermann, S. M. Hayden, and J. Chang, Competing charge, spin, and superconducting orders in underdoped  $\text{YBa}_2\text{Cu}_3\text{O}_y$ , *Phys. Rev. B* **90**, 054514 (2014).
- [13] S. Blanco-Canosa, A. Frano, E. Schierle, J. Porras, T. Loew, M. Minola, M. Bluschke, E. Weschke, B. Keimer, and M. Le Tacon, Resonant x-ray scattering study of charge-density wave correlations in  $\text{YBa}_2\text{Cu}_3\text{O}_{6+x}$ , *Phys. Rev. B* **90**, 054513 (2014).
- [14] T. P. Croft, C. Lester, M. S. Senn, A. Bombardi, and S. M. Hayden, Charge density wave fluctuations in  $\text{La}_{2-x}\text{Sr}_x\text{CuO}_4$  and their competition with superconductivity, *Phys. Rev. B* **89**, 224513 (2014).
- [15] W. Tabis, Y. Li, M. Le Tacon, L. Braicovich, A. Kreyssig, M. Minola, G. Dellea, E. Weschke, M. J. Veit, M. Ramazanoglu, A. I. Goldman, T. Schmitt, G. Ghiringhelli, N. Barišić, M. K. Chan, C. J. Dorow, G. Yu, X. Zhao, B. Keimer, and M. Greven, Charge order and its connection with Fermi-liquid charge transport in a pristine high- $T_c$  cuprate, *Nat. Commun.* **5**, 5875 (2014).
- [16] E. H. da Silva Neto, R. Comin, F. He, R. Sutarto, Y. Jiang, R. L. Greene, G. A. Sawatzky, and A. Damascelli, Charge ordering in the electron-doped superconductor  $\text{Nd}_{2-x}\text{Ce}_x\text{CuO}_4$ , *Science* **347**, 282 (2015).
- [17] R. Comin, R. Sutarto, E. H. da Silva Neto, L. Chauviere, R. Liang, W. N. Hardy, D. A. Bonn, F. He, G. A. Sawatzky, and A. Damascelli, Broken translational and rotational symmetry via charge stripe order in underdoped  $\text{YBa}_2\text{Cu}_3\text{O}_{6+y}$ , *Science* **347**, 1335 (2015).
- [18] R. Comin, R. Sutarto, F. He, E. H. da Silva Neto, L. Chauviere, A. Fraño, R. Liang, W. N. Hardy, D. A. Bonn, Y. Yoshida, H. Eisaki, A. J. Achkar, D. G. Hawthorn, B. Keimer, G. A. Sawatzky, and A. Damascelli, Symmetry of charge order in cuprates, *Nat. Mater.* **14**, 796 (2015).
- [19] E. M. Forgan, E. Blackburn, A. T. Holmes, A. K. R. Briffa, J. Chang, L. Bouchenoire, S. D. Brown, R. Liang, D. Bonn, W. N. Hardy, N. B. Christensen, M. v. Zimmermann, M. Hücker, and S. M. Hayden, The microscopic structure of charge density waves in underdoped  $\text{YBa}_2\text{Cu}_3\text{O}_{6.54}$  revealed by x-ray diffraction, *Nat. Commun.* **6**, 10064 (2015).
- [20] T. Wu, H. Mayaffre, S. Krämer, M. Horvatić, C. Berthier, W. N. Hardy, R. Liang, D. A. Bonn, and M.-H. Julien, Incipient charge order observed by NMR in the normal state of  $\text{YBa}_2\text{Cu}_3\text{O}_y$ , *Nat. Commun.* **6**, 6438 (2015).
- [21] Y. Y. Peng, M. Salluzzo, X. Sun, A. Ponti, D. Betto, A. M. Ferretti, F. Fumagalli, K. Kummer, M. Le Tacon, X. J. Zhou, N. B. Brookes, L. Braicovich, and G. Ghiringhelli, Direct observation of charge order in underdoped and optimally doped  $\text{Bi}_2(\text{Sr,L a})_2\text{CuO}_{6+\delta}$  by resonant inelastic x-ray scattering, *Phys. Rev. B* **94**, 184511 (2016).

- [22] W. Tabis, B. Yu, I. Bialo, M. Bluschke, T. Kolodziej, A. Kozłowski, E. Blackburn, K. Sen, E. M. Forgan, M. v. Zimmermann, Y. Tang, E. Weschke, B. Vignolle, M. Hepting, H. Gretarsson, R. Sutarto, F. He, M. Le Tacon, N. Barišić, G. Yu, and M. Greven, Synchrotron x-ray scattering study of charge-density-wave order in  $\text{HgBa}_2\text{CuO}_{4+\delta}$ , *Phys. Rev. B* **96**, 134510 (2017).
- [23] T. Wu, H. Mayaffre, S. Krämer, M. Horvatć, C. Berthier, W. N. Hardy, R. Liang, D. A. Bonn, and M.-H. Julien, Magnetic-field-induced charge-stripe order in the high-temperature superconductor  $\text{YBa}_2\text{Cu}_3\text{O}_y$ , *Nature (London)* **477**, 191 (2011).
- [24] T. Wu, H. Mayaffre, S. Krämer, M. Horvatić, C. Berthier, P. L. Kuhns, A. P. Reyes, R. Liang, W. N. Hardy, D. A. Bonn, and M.-H. Julien, Emergence of charge order from the vortex state of a high-temperature superconductor, *Nat. Commun.* **4**, 2113 (2013).
- [25] D. LeBoeuf, S. Krämer, W. N. Hardy, R. Liang, D. A. Bonn, and C. Proust, Thermodynamic phase diagram of static charge order in underdoped  $\text{YBa}_2\text{Cu}_3\text{O}_y$ , *Nat. Phys.* **9**, 79 (2013).
- [26] S. Gerber, H. Jang, H. Nojiri, S. Matsuzawa, H. Yasumura, D. A. Bonn, R. Liang, W. N. Hardy, Z. Islam, A. Mehta, S. Song, M. Sikorski, D. Stefanescu, Y. Feng, S. A. Kivelson, T. P. Devereaux, Z.-X. Shen, C.-C. Kao, W.-S. Lee, D. Zhu, and J.-S. Lee, Three-dimensional charge density wave order in  $\text{YBa}_2\text{Cu}_3\text{O}_{6.67}$  at high magnetic fields, *Science* **350**, 949 (2015).
- [27] J. Chang, E. Blackburn, O. Ivashko, A. T. Holmes, N. B. Christensen, M. Hücker, R. Liang, D. A. Bonn, W. N. Hardy, U. Rütt, M. v. Zimmermann, E. M. Forgan, and S. M. Hayden, Magnetic field controlled charge density wave coupling in underdoped  $\text{YBa}_2\text{Cu}_3\text{O}_{6+x}$ , *Nat. Commun.* **7**, 11494 (2016).
- [28] H. Jang, W.-S. Lee, H. Nojiri, S. Matsuzawa, H. Yasumura, L. Nie, A. V. Maharaj, S. Gerber, Y.-J. Liu, A. Mehta, D. A. Bonn, R. Liang, W. N. Hardy, C. A. Burns, Z. Islam, S. Song, J. Hastings, T. P. Devereaux, Z.-X. Shen, S. A. Kivelson, C.-C. Kao, D. Zhu, and J.-S. Lee, Ideal charge density wave order in the high-field state of superconducting YBCO, *Proc. Natl. Acad. Sci. U.S.A.* **113**, 14645 (2016).
- [29] J. Choi, O. Ivashko, E. Blackburn, R. Liang, D. A. Bonn, W. N. Hardy, A. T. Holmes, N. B. Christensen, M. Hücker, S. Gerber, O. Gutowski, U. Rütt, M. v. Zimmermann, E. M. Forgan, S. M. Hayden, and J. Chang, Spatially inhomogeneous competition between superconductivity and the charge density wave in  $\text{YBa}_2\text{Cu}_3\text{O}_{6.67}$ , *Nat. Commun.* **11**, 990 (2020).
- [30] H.-H. Kim, S. M. Souliou, M. E. Barber, E. Lefrançois, M. Minola, M. Tortora, R. Heid, N. Nandi, R. A. Borzi, G. Garbarino, A. Bosak, J. Porras, T. Loew, M. König, P. J. W. Moll, A. P. Mackenzie, B. Keimer, C. W. Hicks, and M. Le Tacon, Uniaxial pressure control of competing orders in a high-temperature superconductor, *Science* **362**, 1040 (2018).
- [31] H.-H. Kim, E. Lefrançois, K. Kummer, R. Fumagalli, N. B. Brookes, D. Betto, S. Nakata, M. Tortora, J. Porras, T. Loew, M. E. Barber, L. Braicovich, A. P. Mackenzie, C. W. Hicks, B. Keimer, M. Minola, and M. Le Tacon, Charge density waves in  $\text{YBa}_2\text{Cu}_3\text{O}_{6.67}$  probed by resonant x-ray scattering under uniaxial compression, *Phys. Rev. Lett.* **126**, 037002 (2021).
- [32] I. Vinograd, S. M. Souliou, A.-A. Haghighirad, T. Lacmann, Y. Caplan, M. Frachet, M. Merz, G. Garbarino, Y. Liu, S. Nakata, K. Ishida, H. M. L. Noad, M. Minola, B. Keimer, D. Orgad, C. W. Hicks, and M. Le Tacon, Using strain to uncover the interplay between two- and three-dimensional charge density waves in high-temperature superconducting  $\text{YBa}_2\text{Cu}_3\text{O}_y$ , *Nat. Commun.* **15**, 3277 (2024).
- [33] O. Zachar, S. A. Kivelson, and V. J. Emery, Landau theory of stripe phases in cuprates and nickelates, *Phys. Rev. B* **57**, 1422 (1998).
- [34] E. Demler and S. Sachdev, Competing orders in thermally fluctuating superconductors in two dimension, *Phys. Rev. B* **69**, 144504 (2004).
- [35] K. B. Efetov, H. Meier, and C. Pépin, Pseudogap state near a quantum critical point, *Nat. Phys.* **9**, 442 (2013).
- [36] L. E. Hayward, D. G. Hawthorn, R. G. Melko, and S. Sachdev, Angular fluctuations of a multicomponent order describe the pseudogap of  $\text{YBa}_2\text{Cu}_3\text{O}_{6+x}$ , *Science* **343**, 1336 (2014).
- [37] L. Nie, L. E. Hayward Sierens, R. G. Melko, S. Sachdev, and S. A. Kivelson, Fluctuating orders and quenched randomness in the cuprates, *Phys. Rev. B* **92**, 174505 (2015).
- [38] Y. Caplan, G. Wachtel, and D. Orgad, Long-range order and pinning of charge-density waves in competition with superconductivity, *Phys. Rev. B* **92**, 224504 (2015).
- [39] Y. Caplan and D. Orgad, Dimensional crossover of charge-density wave correlations in the cuprates, *Phys. Rev. Lett.* **119**, 107002 (2017).
- [40] A. J. Achkar, X. Mao, C. McMahan, R. Sutarto, F. He, R. Liang, D. A. Bonn, W. N. Hardy, and D. G. Hawthorn, Impact of quenched oxygen disorder on charge density wave order in  $\text{YBa}_2\text{Cu}_3\text{O}_{6+x}$ , *Phys. Rev. Lett.* **113**, 107002 (2014).
- [41] N. H. Andersen, M. von Zimmermann, T. Frello, M. Käll, D. Mønster, P.-A. Lindgård, J. Madsen, T. Niemöller, H. F. Poulsen, O. Schmidt, J. R. Schneider, Th. Wolf, P. Dosanjh, R. Liang, and W. N. Hardy, Superstructure formation and the structural phase diagram of  $\text{YBa}_2\text{Cu}_3\text{O}_{6+x}$ , *Physica C* **317-318**, 259 (1999).
- [42] F. Rullier-Albenque, H. Alloul, and R. Tourbot, Disorder and transport in cuprates: weak localization and magnetic contributions, *Phys. Rev. Lett.* **87**, 157001 (2001).
- [43] D. Podolsky and S. Sachdev, Spectral functions of the Higgs mode near two-dimensional quantum critical points, *Phys. Rev. B* **86**, 054508 (2012).